Tuning rf-SQUID flux qubit system's potential with magnetic flux bias*

Hua Tao(花 涛)[a], Xu Wei-Wei(许伟伟)[a)†], Shi Jian-Xin(史建新)[a)], An De-Yue(安德越)[a)], Sun Guo-Zhu(孙国柱)[a)], Yu Yang(于 扬)[b)], and Wu Pei-Heng(吴培亨)[a)]

[a)] *Research Institute of Superconductor Electronics, School of Electronic Science and Engineering, Nanjing University, Nanjing* 210093, *China*

[b)] *National Laboratory of Solid State Microstructures, School of Physics, Nanjing University, Nanjing* 210093, *China*

(Received 6 April 2012; revised manuscript received 17 May 2012)

At an extremely low temperature of 20 mK, we measured loop current in a tunable rf superconducting quantum interference device (SQUID) with a dc-SQUID. By adjusting the magnetic flux applied to the rf-SQUID loop ($\Phi_{\rm f}$) and the small dc-SQUID ($\Phi_{\rm f}^{\rm cjj}$), respectively, the potential shape of the system can be fully controlled *in situ*. Variations of transition step and overlap size in switching current with the barrier flux bias are analyzed, from which we can obtain some relevant device parameters and built up a model to explain the experimental phenomenon.

Keywords: rf-SQUID, potential, flux qubit

PACS: 85.25.Dq, 85.25.Cp, 03.67.Lx **DOI:** 10.1088/1674-1056/21/9/098501

1. Introduction

Superconducting qubits are solid-state qubits and their parameters can be designed and adjusted continuously in a large range. Modern technology allows many options to couple the qubits.[1] So far there are three basic types of superconducting Josephson devices: charge qubit, phase qubit, and flux qubit.[2−5] Recently, many efforts have been made to realize solid-state qubits by improving designs, circuits, and materials to increase the decoherence time.[6,7] The flux qubit has shown the longest decoherence time among all three superconducting types.[8] One of the key critical processes of quantum information is to realize more closely coupled qubits. Recently, Sun *et al.*[9] reported the creation and coherent manipulation of quantum states in a tripartite quantum system. The tunability and coupling of the qubit becomes more and more important in a multiple qubit configuration to realize a quantum computer. In our experiment, we focus on the rf-SQUID flux qubit. The parameter $\beta_{\rm L}$ of rf-SQUID flux qubit is an important parameter of the device and directly related to the barrier height of the system. Connecting two superconducting Josephson junctions with the same parameters in parallel can be equivalent to a single Josephson junction. In this way, one can create $\beta_{\rm L}$ adjustable rf-SQUID flux qubit. The flexibility can be greatly enhanced, and much more work can be done with this type of rf-SQUID flux qubit, both theoretically and experimentally.[10−12] In our experiment, we fully controlled the rf-SQUID flux qubit's potential with a magnetic flux bias. We present detailed rf-SQUID characteristics for different $\beta_{\rm L}$, and explain the intrinsic physics of the connection between the transition step as well as the overlap size and the barrier flux bias.

2. Caculation of qubit energy level

An rf-SQUID qubit consists of a superconducting loop with inductance L interrupted by a single Josephson junction with a fixed critical current $I_{\rm c}$ and capacitance C (see Figs. 1 and 2). To improve the design, we can replace the single junction with a flux-biased and low-inductance dc-SQUID to reach an effectively tunable $I_{\rm c}$. Here, we assume the two junctions in the small dc-SQUID loop have the same fabrication pa-

*Project supported by the National Basic Research Program of China (Grant Nos. 2011CBA00107 and 2011CBA00202) and the National Natural Science Foundation of China (Grant Nos. 61027008 and 11074114).

†Corresponding author. E-mail: wwxu@nju.edu.cn

© 2012 Chinese Physical Society and IOP Publishing Ltd

rameters, i.e., each with a capacitance $C/2$ and a critical current $I_{c0}/2$. Then this system is identical to a simple rf-SQUID with capacitance C and critical current $I_c = I_{c0}|\cos(\pi\Phi_f^{cjj}/\Phi_0)|$, which shows that the critical current is effectively modulated by an external flux bias Φ_f^{cjj}. Here, $\Phi_f^{cjj} = M_f^{cjj}V_{pb}/R_1$, Φ_0 is the flux quantum, M_f^{cjj} is the mutual inductance between barrier flux bias coil 1 and the small dc-SQUID loop, V_{pb} is the voltage in coil 1, and R_1 is the resistance of coil 1.

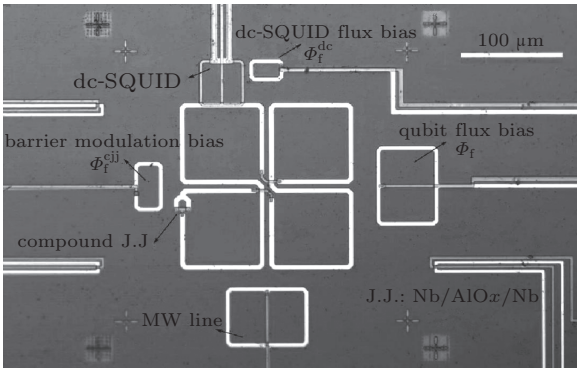


Fig. 1. Optical micrograph of an rf-SQUID sample.

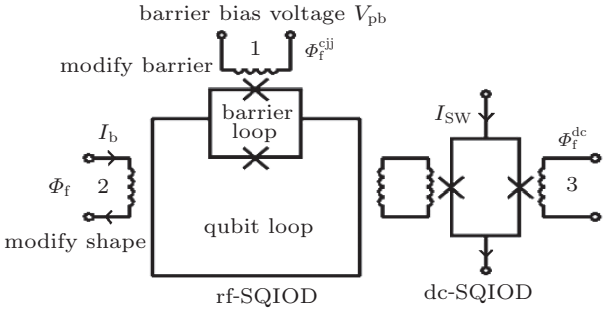


Fig. 2. Schematic of the manipulation and measurement of the system. The crosses represent the Josephson junctions.

The dynamics of rf-SQUID qubit can be described in terms of a variable Φ and is identical to that of a particle with mass C and kinetic energy $C\dot{\Phi}^2/2$ moving in the potential well. The potential $U(\Phi)$ reads

$$U(\Phi) = U_0\left[\frac{1}{2}\left(\frac{2\pi(\Phi-\Phi_f)}{\Phi_0}\right)^2 - \beta_L\cos\left(\frac{2\pi\Phi}{\Phi_0}\right)\right], \quad (1)$$

where $U_0 \equiv \Phi_0^2/(4\pi^2 L)$, and $\beta_L = 2\pi I_c L/\Phi_0$. When an external magnetic flux Φ_f close to $\Phi_0/2$ is applied to the qubit loop, the potential as a function of flux Φ has two wells separated by a potential barrier. The two potential wells correspond to two distinct macroscopic flux states ($|L\rangle$ and $|R\rangle$) with screening currents circulating in different directions. Especially at $\Phi_f = 0.5\Phi_0$, the double-well potential is symmetric and the screening currents circulating in opposite directions have equal magnitude. The flux states can be detected by an inductively coupled dc-SQUID magnetometer. By changing the qubit flux bias Φ_f , one can tilt the double-well potential, i.e., change the energy difference ε (shown in Fig. 3) between the two potential wells. Adjusting Φ_f^{cjj} (V_{pb}) can modulate I_c (β_L), and therefore control the barrier height ΔU (shown in Fig. 3).

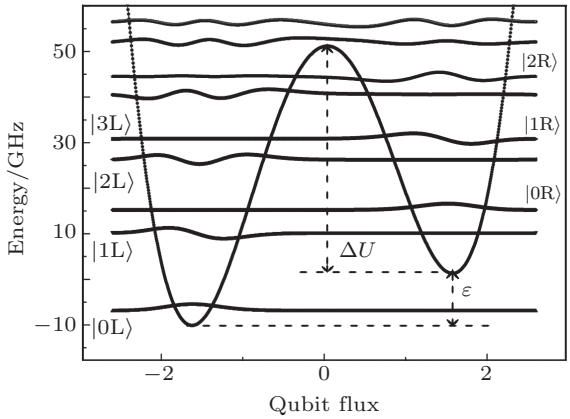


Fig. 3. Calculated energy levels and wavefunctions of an rf-SQUID system at flux detuning $\delta\Phi_f = \Phi_f$–$0.5\Phi_0 = -7.5 \times 10^{-3}\Phi_0$ with $L = 1080$ pH, $C = 80$ fF, and $\beta_L = 1.6$. The level spacing between $|0L\rangle$ and $|1L\rangle$ is about 17 GHz. The ΔU is the barrier height, and ε is the energy difference between two wells.

The system has several quantized energy levels that are below the barrier top and localized in either left well or right well. The levels localized in the left well correspond to the flux state $|L\rangle$; the levels localized in the right well correspond to the flux state $|R\rangle$. Above the barrier top, there are also some energy levels not localized in either potential well. To make this point more clear quantitatively, we use the Fourier Grid Hamiltonian (FGH) method[13] to calculate the energy levels and the corresponding wavefunctions for flux detuning $\delta\Phi_f = \Phi_f$–$0.5\Phi_0 = -7.5 \times 10^{-3}\Phi_0$ with $L = 1080$ pH, $C = 80$ fF, and $\beta_L = 1.6$. The results are shown in Fig. 3. The wavefucntions of four energy states $|0L\rangle$, $|1L\rangle$, $|2L\rangle$, and $|3L\rangle$ are localized in the left well, while those of three states $|0R\rangle$, $|1R\rangle$, and $|2R\rangle$ are localized in the right well. Two energy levels are above the potential barrier top, and their wavefunctions span over both wells, which are usually referred to as the common levels.

3. Experiment and analysis

Our samples are Nb/AlOx/Nb junctions fabricated on an oxidized Si substrate using the standard

trilayer process (see Fig. 1). Some of the device parameters are: rf-SQUID loop inductance $L \approx 1.3$ nH, junction capacitance $C \approx 35$ fF, and junction critical current $I_c \approx 610$ nA. The schematic of the manipulation and measurement of the system is shown in Fig. 2. Two on-chip current bias lines (coil 1 and coil 2) transfer the magnetic flux to the rf-SQUID loop (Φ_f) and the small dc-SQUID loop (Φ_f^{cjj}), detuning the potential from symmetric point and modulating the potential barrier height, respectively. Therefore, we can control two degrees of freedom of the system potential *in situ* by adjusting Φ_f and Φ_f^{cjj}.

The rf-SQUID flux state is detected by an underdamped dc-SQUID magnetometer with a hysteretic current–voltage curve inductively coupled to the qubit loop. First, we give a brief introduction on how to measure the switching current in the experiment. We slowly sweep the dc-SQUID bias current in triangle waveform and monitor the voltage across the dc-SQUID. When the junction switches to the voltage state, the counter records the switching current value (actually switching time). The junction will return to zero-voltage state at the end of one triangle signal. After making this measurement repeatedly (with a repetition frequency of 71.3 Hz), we can obtain the distribution of the switching current (shown in Fig. 4). The self inductance of the dc-SQUID magnetometer loop is about 120 pH. An external flux bias line placed about 5 μm away from the dc-SQUID magnetometer loop is used to exert a magnetic flux to it. We can easily obtain the switching current of the dc-SQUID magnetometer as a function of the flux bias Φ_f^{dc}. The dc-SQUID is biased at the point where it is most sensitive to the external magnetic field. From the modulation periodicity (0.99 mA), we can obtain the mutual inductance between the dc-SQUID loop and the current bias line 3, which is about 2.09 pH.

To make the rf-SQUID loop insensitive to the ambient flux noise as well as cross talk between the two bias fluxes, the rf-SQUID loop is designed with a second order gradiometric configuration. No net flux is coupled to the gradiometer by a spatially uniform field. The only response of the SQUID is the spatial variation of the magnetic field. If Φ_f is close to $0.5\Phi_0$, the direction of the rf-SQUID current is reversed, causing a transition step in switching current of the dc-SQUID magnetometer. Thus, the magnitude of the transition step is exactly the magnitude of the qubit signal. The qubit signal can be identified by sweeping Φ_f while measuring the switching current of the dc-SQUID. We can see some qubit signals in Fig. 5. The qubit signal spacing is about 1.87 mA, corresponding to one flux quantum ($\Phi_0 = 2.07 \times 10^{-15}$ Wb) through the rf-SQUID loop. Thus, we can obtain the mutual inductance between the rf-SQUID loop and the qubit flux bias, namely ∼1.16 pH. The mutual inductance between the dc-SQUID and rf-SQUID loops is about 23.4 pH, almost equal to that calculated by FastHenry. Once the qubit transition step region is identifed, we can also apply a pulsed current to the dc-SQUID magnetometer to read out the qubit signal more quickly. The readout pulse consists of a 15-ns sampling current (rising time: ∼10 ns) having almost the same amplitude as the critical current and a 15-μs holding current (holding plateau: ∼10 μs) which is higher than the retrapping current of the dc-SQUID magnetometer in amplitude.

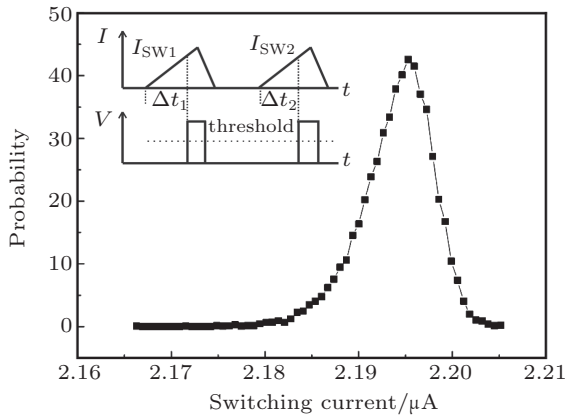


Fig. 4. Distribution of the switching current of the dc-SQUID magnetometer. The mean I_{SW} is 2.186 μA, the standard deviation is 10 nA. The inset shows the measurement sequence of switching current.

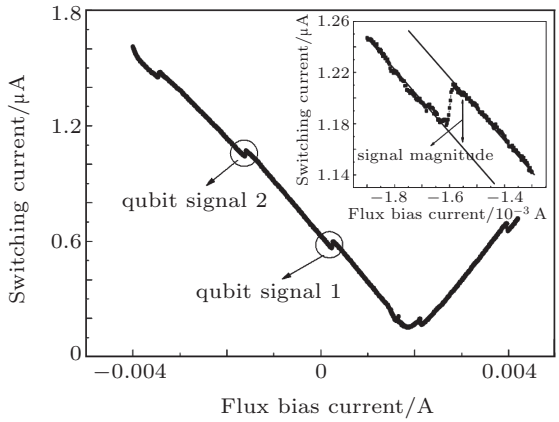


Fig. 5. Qubit signals. The inset shows the detail of the qubit signal. The transition step is the amplification of the qubit signal.

Since the critical current is proportional to the Josephson coupling energy, the amplitude of the cir-

culation current in the rf-SQUID loop can be effectively modulated by an external flux $\Phi_{\rm f}^{\rm cjj}$, supplied by a coil placed about 12 μm away from the compound junction and the mutual inductance is about 0.4 pH. We can adjust the barrier bias voltage $V_{\rm pb}$ to modulate the potential-barrier height of the rf-SQUID. The shift (qubit step) of the dc-SQUID switching curve can be used to study the rf-SQUID characteristics by sweeping slowly the rf-SQUID flux bias and collecting all of the corresponding switching curves of the SQUID. The detailed view of qubit steps with eight different potential barrier heights (corresponding to different barrier flux biases $\Phi_{\rm f}^{\rm cjj}$) is shown in Fig. 6, which reflects the characteristics of the rf SQUID with different values of the parameter $\beta_{\rm L}$. The data are shifted vertically for clear demonstration.

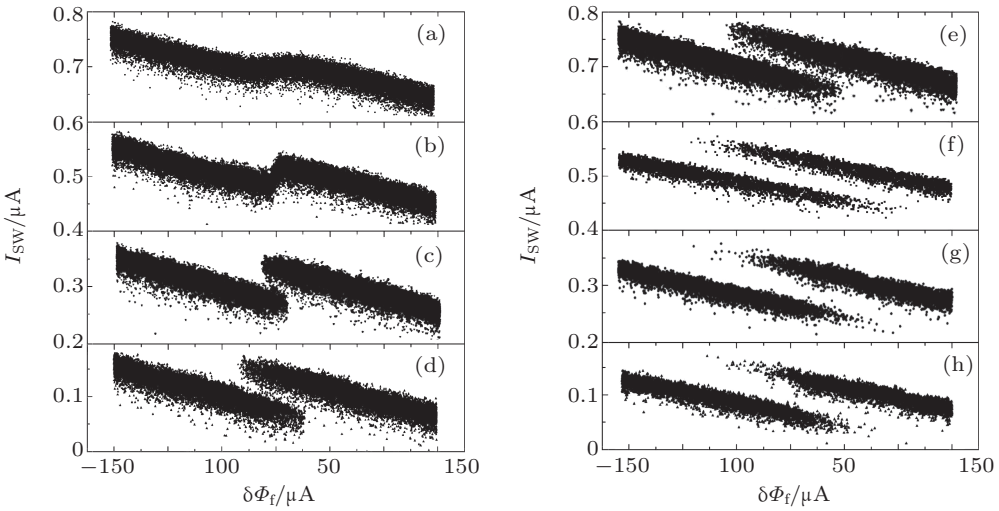


Fig. 6. Characteristics of rf SQUID for different values of $\beta_{\rm L}$ for (a) $\Phi_{\rm f}^{\rm cjj} = 0.77\Phi_0$, (b) $0.80\Phi_0$, (c) $0.85\Phi_0$, (d) $0.90\Phi_0$, (e) $0.95\Phi_0$, (f) $1.00\Phi_0$, (g) $1.05\Phi_0$, and (h) $1.10\Phi_0$. The $I_{\rm sw}$ denotes the switching current.

A double rf SQUID shows a hysteretic flux-in/flux-out characteristic, and has jumps between different potential wells. From Fig. 6 we can see that as the barrier height or $\beta_{\rm L}$, increases, the magnitude of qubit signal (switching current longitudinal splitting) increases. The origin of this phenomenon is that when the barrier flux bias increases, the rf SQUID with its current circulating around the loop in clockwise and counterclockwise directions becomes larger accordingly. Therefore, the transition step magnitude in the switching current of the dc-SQUID magnetometer also increases. The qubit signal magnitude as a function of the barrier flux bias is shown in Fig. 7. It shows a sharp increase of the magnitude of qubit signal when the barrier flux bias changes from $0.75\Phi_0$ to $0.90\Phi_0$, and a slight increase when the flux bias changes from $0.90\Phi_0$ to Φ_0. From Φ_0 to $1.10\Phi_0$, the magnitude of qubit signal is nearly constant. This can be caused by the hysteresis characteristics of the rf SQUID. The maximal magnitude of qubit signal is about 70 nA.

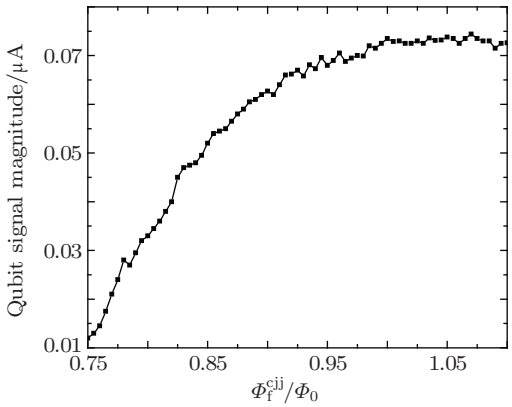


Fig. 7. Qubit signal magnitude as a function of the barrier flux bias.

From Fig. 6, we can also see that as the barrier height increases, i.e., $\beta_{\rm L}$ becomes larger, the magnitude of switching current horizontal overlap (hysteresis width) increases. The underlying physics is that when the potential barrier is low ($\beta_{\rm L}$ is small), both the left and right potential wells are shallow. In this case, small flux detuning can affect the system's stability. Variation of the potential-well symmetry by tuning $\Phi_{\rm f}$ is in a very small range around $\Phi_{\rm f} = 0.5\Phi_0$.

If the potential barrier is high ($\beta_{\rm L}$ is large), both the left and right potential wells are deep, and the states in each well are more complex. Variation of the potential-well symmetry is in a larger range around $\Phi_{\rm f} = 0.5\Phi_0$, and the system has a greater probability to tunnel through the barrier and reach a state in another well compared with the case that the potential barrier is low. The switching current horizontal overlap magnitude as a function of the barrier flux bias is shown in Fig. 8. We can see that the overlap width is maximal when the barrier flux bias is a special integer number of flux quanta. It decreases symmetrically as the flux increases or decreases from one of these values. Figure 8 shows that the horizontal overlap magnitude increases when the barrier bias voltage changes from $0.75\Phi_0$ to Φ_0, and decreases when the voltage changes from Φ_0 to $1.10\Phi_0$. The maximal magnitude of the horizontal overlap is about 135 mΦ_0.

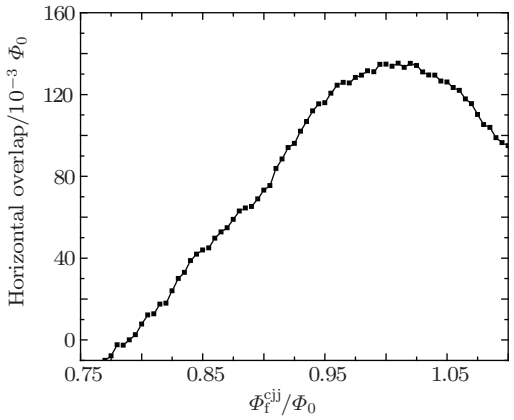


Fig. 8. Switching current horizontal overlap magnitude as a function of the barrier flux bias.

4. Computer simulation

We define i=$F(\Phi_{\rm f})$ to describe the relationship between the external magnetic flux threading the qubit loop and the macroscopic current circulating the loop by. The relationship changes with the potential barrier height ($\beta_{\rm L}$). In view of magnetic flux quantization, we can obtain the relationship between Φ and Φ_0 as

$$\frac{\delta}{2\pi}\Phi_0 + \Phi = N\Phi_0, \tag{2}$$

where Φ is the effective magnetic flux threading the quibit loop, δ is the phase difference of the two sides of the equivalent junction, and N is an integer number. Using Josephson equation, we can obtain

$$i = I_{\rm c}\sin\delta = I_{\rm c}\sin\frac{-2\pi\Phi}{\Phi_0} = -I_{\rm c}\sin\frac{2\pi\Phi}{\Phi_0}. \tag{3}$$

The effective magnetic flux Φ which threads the qubit loop is composed of the external magnetic flux $\Phi_{\rm f}$ and the self-inductance current magnetic flux iL. Thus, we obtain

$$\Phi = \Phi_{\rm f} + iL = \Phi_{\rm f} - I_{\rm c}L\sin\frac{2\pi\Phi}{\Phi_0}. \tag{4}$$

Given that $\beta_{\rm L} = 2\pi I_{\rm c}L/\Phi_0$, using Eqs. (3) and (4), we obtain

$$\frac{2\pi iL}{\Phi_0} = -\beta_{\rm L}\sin\frac{2\pi\Phi}{\Phi_0}, \tag{5}$$

$$\frac{2\pi\Phi}{\Phi_0} = \frac{2\pi\Phi_{\rm f}}{\Phi_0} - \beta_{\rm L}\sin\frac{2\pi\Phi}{\Phi_0}. \tag{6}$$

Using Eqs. (5) and (6), we can calculate the relationship $i = F(\Phi_{\rm f})$, as shown in Fig. 9.

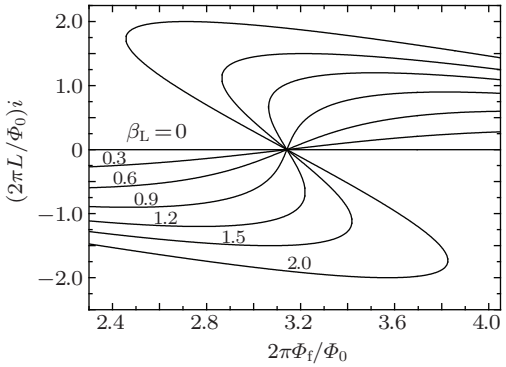


Fig. 9. Simulation results of the relationship between the external magnetic flux threading the qubit loop and the macroscopic current circulating the loop for different $\beta_{\rm L}$.

In Fig. 9, when $\beta_{\rm L} < 1$, the curve is single-valued; when $\beta_{\rm L} > 1$, there are three values of i corresponding to one value of $\Phi_{\rm f}$. The upper and lower values are in steady state and the middle one is unstable. As $\beta_{\rm L}$ becomes larger, we can also see both the horizontal overlap and the longitudinal splitting of the curves become larger. All of these results agree with the experimental observations well.

5. Conclusion

In our experiment, we controlled the magnetic flux bias of the rf-SQUID qubit loop ($\Phi_{\rm f}$), which determines the asymmetry of the potential, and the magnetic flux bias of a small dc-SQUID ($\Phi_{\rm f}^{\rm cjj}$), which modulates the potential barrier height. We analyzed and explained the dependence of the qubit signal magnitude and switching current horizontal overlap on the barrier flux bias. The simulation model matches the experiment phenomenon well. On this basis, the best parameter area for barrier controlling can be obtained.

References

[1] Nakamura Y, Pushkin Y A and Tsai J S 1999 *Nature* **398** 786

[2] Yu Y, Zhu S, Sun G Z, Wen X D, Dong N, Chen J, Wu P H and Han S Y 2008 *Phys. Rev. Lett.* **101** 157001

[3] Cao W H, Yu H F, Tian Y, Yu H W, Ren Y F, Chen G H and Zhao S P 2009 *Chin. Phys.* B **18** 5044

[4] Liang B L, Wang J S, Meng X G and Su J 2010 *Chin. Phys.* B **19** 010315

[5] Ji Y H, Lai H F, Cai S H and Wang Z S 2010 *Chin. Phys.* B **19** 030310

[6] Astafiev O, Pashkin Y A, Nakamura Y, Yamamoto T and Tsai J S 2004 *Phys. Rev. Lett.* **93** 267007

[7] McDermott R 2009 *IEEE Trans. Appl. Supercond.* **19** 2

[8] Bylander J, Gustavsson S, Yan F, Yoshihara F, Harrabi K, Fitch G, Cory D G, Nakamura Y, Tsai J S and Oliver W D 2011 *Nature Phys.* **7** 565

[9] Sun G Z, Wen X D, Mao B, Chen J, Yu Y, Wu P H and Han S Y 2010 *Nature Commun.* **1** 51

[10] Deng H, Yu H F, Xue G M, Tian Y, Ren J K, Wu Y L, Huang K Q, Zhao S P and Zheng D N 2012 *Chin. Phys.* B **21** 040307

[11] Cong S H, Wang Y W, Sun G Z, Chen J, Yu Y and Wu P H 2011 *Chin. Phys.* B **20** 050316

[12] Chiorescu I, Nakamura Y, Harmans C J P M and Mooij J E 2003 *Science* **299** 1869

[13] Semay C 2000 *Phys. Rev.* E **62** 8777